今日の治療指針

私はこう治療している

総編集
山口　徹　北原光夫　福井次矢

TODAY'S THERAPY 2012

原発性・転移性肝腫瘍（内科）

primary and secondary liver tumor (medical treatment)

佐々木　裕　熊本大学大学院教授・消化器内科学

病態と診断

肝臓に発生する腫瘍は，悪性腫瘍と良性腫瘍に分けられる．さらに前者は大別すると原発性肝癌と転移性肝腫瘍に分類される．原発性肝癌の内訳は，90%以上を肝細胞癌が占め，肝内胆管癌が4%程度であり，ほかに混合型肝癌や胆管嚢胞腺癌，肝芽腫などが含まれるが，それらの頻度はいずれも1%未満である．

肝細胞癌の特徴として，その多くが慢性肝疾患を基礎疾患として有していることが挙げられる．すなわち，肝細胞癌患者の約70%はC型肝炎ウイルス（HCV）陽性肝硬変・慢性肝炎を，約15%はB型肝炎ウイルス（HBV）陽性肝硬変・慢性肝炎を有している．このように慢性肝疾患患者は肝細胞癌の高危険群であり，なかでも肝硬変に至ると超高危険群とされている．

したがってこれらの患者群を囲い込み，厳密に経過観察することで肝細胞癌の早期発見が可能となる．実際に高危険群では6か月ごとの超音波検査と腫瘍マーカー（AFP・AFP-L3分画*1・PIVKA-II）の測定が推奨されており，さらに超高危険群では3-4か月ごとの超音波検査と腫瘍マーカーの測定と6-12か月ごとのダイナミックCT・MRIが推奨されている（*1 AFP-L3分画は肝細胞癌の病名がないと保険適用がない）．最近ではウイルス性慢性肝疾患やアルコール性肝硬変以外に，NASH（非アルコール性脂肪性肝炎）患者の一部にも肝細胞癌が発生することが明らかとなり，肝逸脱酵素（ALT，AST）が高い脂肪肝患者も定期的に超音波検査を施行することが勧められている．

仮に経過観察中の超音波検査にて肝内に結節性病変が指摘された場合は，ダイナミックCTあるいはダイナミックMRI検査を行う必要がある．典型的な肝細胞癌は多血性（血管に富んでいる）であるために，動脈相では高吸収（高信号），平衡相では低吸収（低信号）な病変として描出される．ダイナミックCT・MRIで典型的肝細胞癌の所見が得られなかった場合は，2cm以上の病変であれば血管造影下CT（CTAP，CTHA）やSPIO-MRIなどの画像検査，あるいは腫瘍生検を考慮する必要がある．最近では新しい造影剤Gd-EOB-DTPA（EOB・プリモビスト）を使用したMRIや，ソナゾイドを使用した造影エコーの導入により，結節性病変の血流評価に加えて，肝細胞機能評価を加味した画像検査法が，早期肝細胞癌の診断の一助となっている．

肝内胆管癌は肝細胞癌に次いで頻度の高い腫瘍である．HCV陽性率，HBV陽性率はそれぞれ約19%，約6%で，合計しても肝炎ウイルス陽性率は全体の1/4であるがゆえに，肝細胞癌と異なり危険群の囲い込みが困難である．

肝内胆管癌の肉眼型は，腫瘤形成型，胆管浸潤型，胆管内発育型の3型に分類される．造影CT検査において，腫瘤形成型では癌部・非癌部の境界が比較的明瞭であり，早期に腫瘍の辺縁がring上に造影されることが多い．そのため転移性肝癌や肝腫瘍との鑑別が困難である．胆管浸潤型では末梢胆管拡張を伴うことが特徴的である．腫瘍マーカーとしてはCEAやCA19-9が陽性となることが多い．

一方，肝臓の良性腫瘍のなかで肝血管腫は最も頻度が高い．肝血管腫の特徴的所見は，ダイナミックCT・MRI検査にて，病変の辺縁から造影剤に染まり次第に中心部が染まっていくこと，濃染が持続することである．またMRI検査のT1強調画像においては低信号，T2強調画像においては著明な高信号を呈することも特徴として挙げられる．

そのほかに頻度は少ないものの，良性腫瘍として限局性結節性過形成（FNH）や肝細胞腺腫が挙げられる．これらはダイナミックCT・MRI検査の動脈相にて多血性病変として描出されるために，肝細胞癌との鑑別が問題となることがある．なかでもFNHは中心部に存在する異常血管により血流増加が起こり，肝細胞の増生がもたらされることで形成される結節性病変である．特徴的所見としては，血管造影下での車軸状の血管構築である．造影エコーでも腫瘍中心部から辺縁へと広がっていく車軸状の血管構築が描出されるために，最近では診断の一助となっている．一方，肝細胞腺腫は画像所見からでは肝細胞癌との鑑別は困難であるが，肝細胞腺腫は硬変肝に発生することはまれであり，また糖原病や経口避妊薬との関連が報告されているので，そのような患者背景も鑑別の一助となる．

治療方針

Ⓐ 肝細胞癌の治療

1. 治療方針　肝細胞癌は慢性肝疾患を母地として発生するために，たとえ根治的治療を施しても，高率に異時性，異所性再発をきたし予後不良な癌腫である．したがって，治療方針を決定するにあたり，癌の進展度だけでなく，肝臓の予備能も考慮する必要がある．「科学的根拠に基づく肝癌診療ガイドラ

図　日本肝臓学会提唱のコンセンサスに基づく肝細胞癌治療アルゴリズム 2010

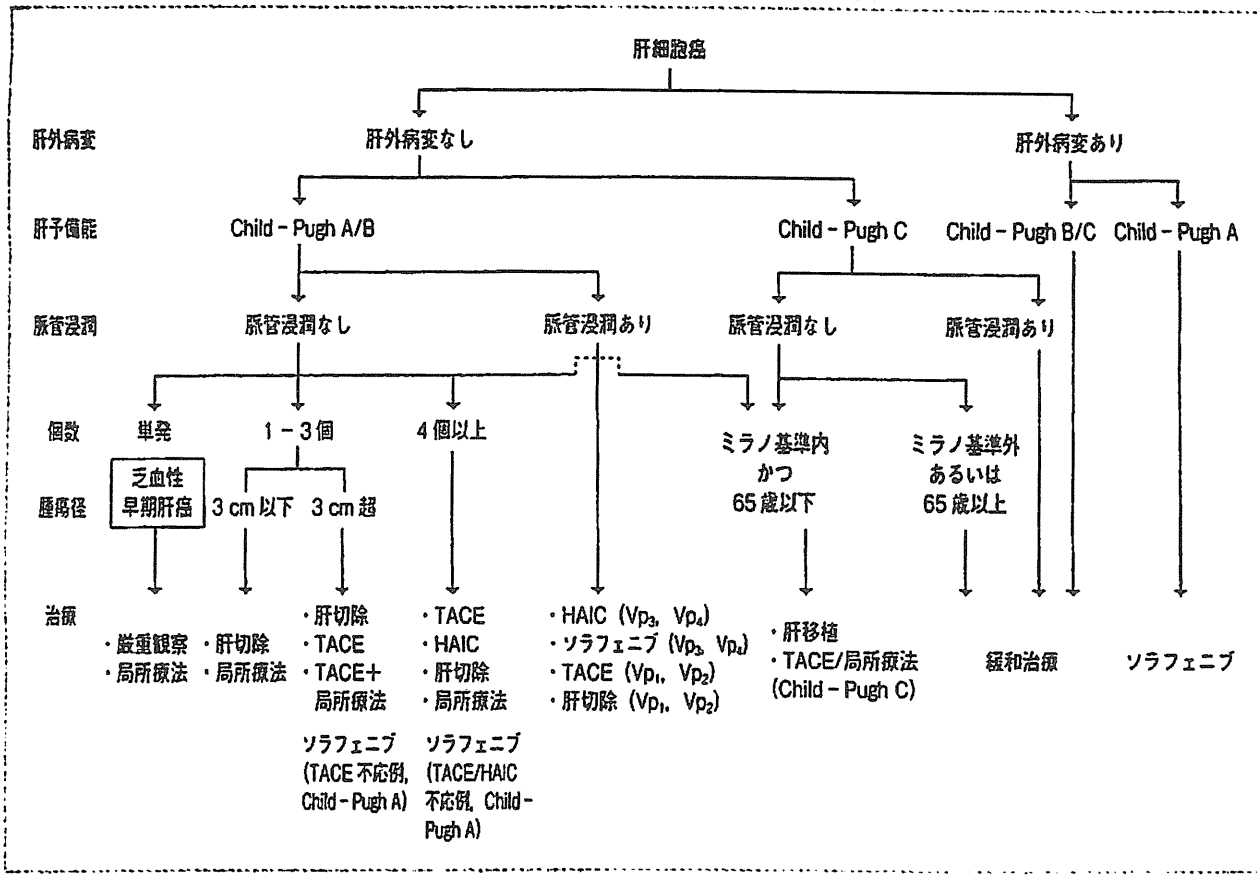

（日本肝臓学会編：肝癌診療マニュアル第2版．p125．医学書院，2010より転載）

イン」では，肝障害度，腫瘍個数，腫瘍径の3つの因子を基にしたアルゴリズムで治療法を選択することが推奨されている（図）．切除の適応がない場合は内科的治療の対象となる．主な治療法として，局所療法（RFA：ラジオ波焼灼療法，PEIT：エタノール注入療法，MCT：マイクロ波凝固療法），肝動脈化学塞栓療法（TACE），肝動注化学療法（HAIC），全身化学療法が挙げられる．

具体的には，切除の適応外で3cm，3個以内の結節であれば，局所療法が推奨される．局所療法の適応とならない場合は，TACEの適応であり，TACE不応例や門脈・静脈・胆管侵襲がある場合は，HAICもしくは全身化学療法を考慮する．肝外転移がある場合は全身化学療法の適応である．肝機能不良例ではそれ自体が予後不良因子であり，また治療後の肝不全のリスクが高く，3cm，3個以内の結節（単結節であれば，5cm以内）が存在する場合は肝移植が考慮されるが，それ以外の積極的治療は推奨されない．

2. 局所治療　局所治療にはRFA，PEIT，MCTが挙げられるが，最近では局所制御の面から多数の施設ではRFAを主体とした局所療法が行われている．局所治療について詳細は他項を参照されたい（「ラジオ波焼灼療法」⇨467頁）．

3. 肝動脈化学塞栓療法（TACE）　TACEはRFAの適応とならない，つまり3cm超の結節や4個以上の病変がある場合に適応となる．基本的には大きさ・個数の制限はないものの，脈管侵襲や肝外転移がある場合は適応外となる．また複数回繰り返しても肝細胞癌の制御が困難な場合は，他治療法を考慮すべきである．具体的な方法については他項を参照されたい（「冠動脈化学塞栓療法」⇨466頁）．

4. 肝動注化学療法（HAIC）　HAICはTACE不応例や脈管侵襲を伴う高度進行例が対象となる．HAICは薬剤を直接，腫瘍の栄養血管から注入することで局所内の抗癌剤濃度を上昇させることが可能であること，また薬剤代謝を担う肝臓を抗癌剤が最初に通過することで全身的な副作用を軽減しうること，この2つの点が有効性と有用性の理論的背景である．HAICは大きく分けて，単回動注法とリザーバーカテーテル留置を必要とする反復動注法があり，下記に処方例を提示する．

a. 単回動注法

Rp 処方例

アイエーコール注　1回 65 mg/m² 生理食塩液 70 mL に溶解して 30 分かけて動注　4－6 週ごとに投与を繰り返す

b. 反復動注法

①低用量 5－FU＋CDDP 療法（Low dose FP 療法）

Rp 処方例

ランダ注　10 mg/body　1時間かけて

その後

5－FU 注　250 mg/body　5時間かけて動注

これを 5 日間連続投与，2 日間休薬し 4 週間で 1 クールとする

②IFN 併用 5－FU 療法（FAIT 療法）

Rp 処方例　下記を併用する．

5－FU 注　500 mg/body　24 時間持続動注を 14 日間連日投与　14 日間休薬

オーアイエフ注　1回 500 万単位　皮下注　週 3 回投与を 4 週間 (保外)

4 週間で 1 クールとする

IFN（インターフェロン）は肝細胞癌にはいまだ保険適用がないため，自費治療となる（2011 年 8 月現在）．

動注化学療法は奏効すると比較的良好な予後が得られることが一般的に知られているが，奏効しない場合の予後は不良のため，漫然と継続すべきでない．

5. 全身化学療法　これまで肝細胞癌に対する有効な全身化学療法は存在しなかったが，分子標的治療薬であるソラフェニブ（ネクサバール）の有効性が欧米において認められ，本邦でも 2009 年 5 月保険適用となった．適応としては，Child－Pugh A と肝機能が保たれた TACE 不応例や遠隔転移例が対象となる．病勢維持を目的とした薬剤であり，腫瘍縮小例は少ない．多彩な副作用を呈することがあるため，使用経験の豊富な医師により投与されるべき薬剤である．

Rp 処方例

ネクサバール錠（200 mg）　4錠　分 2　朝・夕食後

Ⓑ 肝内胆管癌の治療

肝内胆管癌に対する治療は，切除が唯一の根治治療であり，化学療法は切除不能例や術後再発例に行われることが多い．しかし肝内胆管癌に対する化学療法の標準的プロトコールは存在せず，胆道癌で使用されるゲムシタビン（ジェムザール）や TS－1 などの全身投与を行うことが多い．最近では，胆道癌においてゲムシタビンや 5－FU，プラチナ製剤の併用療法の有効性の報告が散見されるようになっており，今後さらに質の高い臨床試験により標準的な治療法が確立されることを期待したい．

Ⓒ 転移性肝癌の治療

転移性肝癌は，原発巣がコントロールされており，肝臓以外に転移がない場合，局所治療の対象となる．転移性肝癌は特に大腸癌，胃癌などの消化器悪性腫瘍からの頻度が高い．転移性肝癌の最も有効な治療法は切除であるが，近年では RFA の有効性が報告され，切除困難例では RFA の適応も検討すべきである．肝臓以外に病変がある場合は，全身化学療法を考慮する．

原発性・転移性肝腫瘍（外科）

primary and secondary liver cancer (surgical treatment)

高山忠利　日本大学教授・消化器外科学

概説 原発性肝癌

わが国の原発性肝癌の 94% は肝細胞癌であり，次いで肝内胆管癌が 4% を占める．その他，胆管嚢胞腺癌，肝芽腫などが続くが，ごく低率である．

病態と診断

Ⓐ 肝細胞癌

肝細胞癌の大半は，B 型（16%），C 型（70%）であるが，近年，原因不明の肝細胞癌が増加傾向にある．

肝炎ウイルス陽性例では感染から約 30 年で発癌し，肝硬変になると発癌率は 7% 程度に上昇すると試算される．慢性肝炎や肝硬変の肝細胞癌ハイリスクグループでは，腹部超音波と α－fetoprotein（特に L3 分画）や PIVKA－II による血液検査，造影剤アレルギーや腎障害などの禁忌がなければ，dynamic CT/MRI を 3－6 か月ごとに行う．

Ⓑ 肝内胆管癌

ハイリスクグループは特定されておらず，進行例を除き症状に乏しい．診断時の腫瘍径 3 cm 以上が 70% 以上を占める．CEA，CA 19－9 などの腫瘍マーカー高値症例では，本疾患を念頭におき，腹部超音波，CT，MRI などの画像診断を行う．画像所見は腺癌に準じ乏血性であるが，末梢の胆管拡張像が特徴的である．肝細胞癌に比べリンパ節転移が多く，切除例で 33% に達し，重要な予後規定因子である．

図　科学的根拠に基づく肝細胞癌治療アルゴリズム 2009

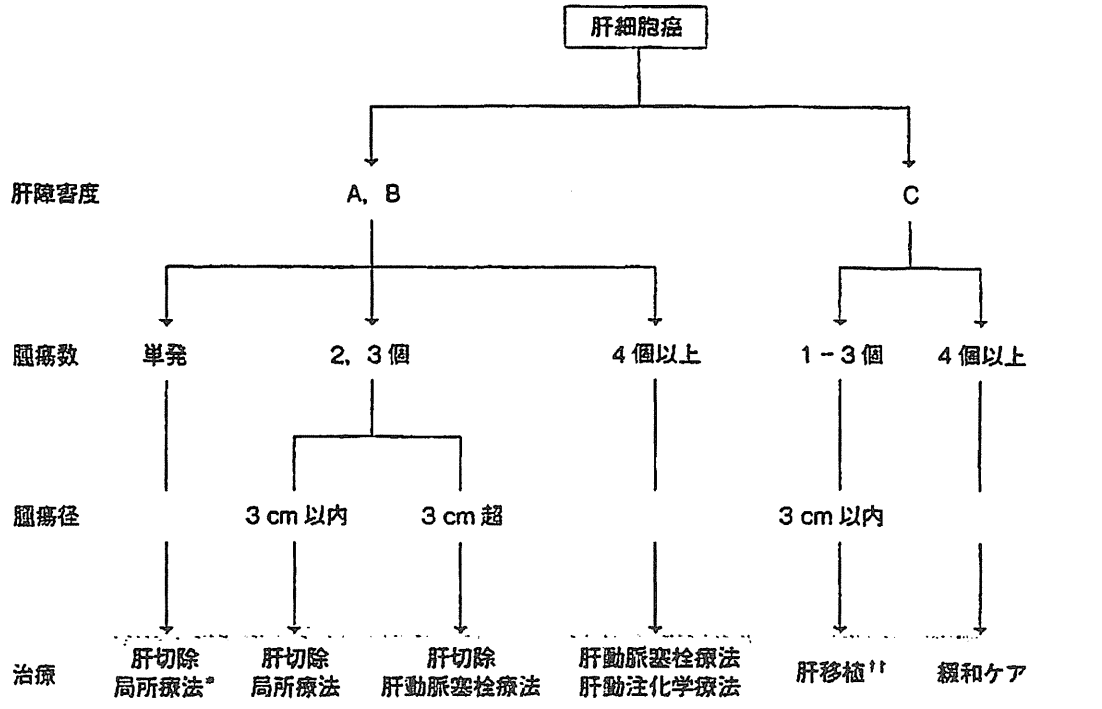

（日本肝臓学会編：科学的根拠に基づく肝癌診療ガイドライン 2009 年版．p13．金原出版．2009 より転載）

治療方針

Ⓐ 肝細胞癌

肝細胞癌では慢性肝炎，肝硬変の合併が高率である．そのため治療に際し，腫瘍進行度に加え肝予備能の制約を受ける．また，比較的早期より脈管浸潤を生じ，肝内に転移しやすい（特に経門脈的進展が多い），背景肝自体が前癌病変とみなしうる状態であり，根治治療後の再発には転移のみならず，多中心性発生による 2 次発癌が関与するという特徴がある．

治療方針については肝細胞癌治療アルゴリズム（図）が一般に利用されている．肝障害度 A，B で腫瘍数 3 個以内が外科的切除の適応であり ICG 15 分停滞率より求められる許容肝切除量を考慮し術式が選択される．

Ⓑ 肝内胆管癌

外科的切除が唯一の根治療法である．しかし，切除例の 5 年生存率は 33% にとどまり，リンパ節陽性例は 16% とさらに低下する．

転移性肝癌

肝はさまざまな悪性腫瘍の転移部位となるが，通常はその疾患の終末像を意味する．外科的切除の対象となるのは大腸癌や神経内分泌系悪性腫瘍，カルチノイドからの肝転移などとなる．胃癌，乳癌などの肝転移なども腫瘍条件によっては手術適応となりうる．

病態と診断

通常，肝機能は正常なため，拡大切除が可能なことが多い．術後の肝再生能も良好なため再切除となる症例も多く，複数回の肝切除を念頭において肝機能を温存するよう術式を選択する．術後再発の頻度が高いため，緻密な経過観察が必要である．

治療方針

大腸癌肝転移に対する肝切除の安全性はすでに確立されており，同時性，異時性を問わず，転移巣の数や大きさにかかわらず，治癒的に切除可能であれば肝切除の適応とされている．肺転移合併症例も肺転移巣が 2－3 個までであれば肝切除の適応である．しかし，肝門や傍大動脈のリンパ節転移が明らかな場合は肝切除の適応とならない．

Biochemical and Biophysical Research Communications 425 (2012) 619–624

Contents lists available at SciVerse ScienceDirect

Biochemical and Biophysical Research Communications

journal homepage: www.elsevier.com/locate/ybbrc

Identification of hepatocyte growth factor activator (Hgfac) gene as a target of HNF1α in mouse β-cells

Tsuyoshi Ohki [a,b], Yoshifumi Sato [a], Tatsuya Yoshizawa [a], Ken-ichi Yamamura [c], Kentaro Yamada [b], Kazuya Yamagata [a,*]

[a] Department of Medical Biochemistry, Faculty of Life Sciences, Kumamoto University, Kumamoto, Japan
[b] Division of Endocrinology and Metabolism, Kurume University School of Medicine, Kurume, Japan
[c] Division of Developmental Genetics, Center for Animal Resources and Development, Institute of Resource Development and Analysis, Kumamoto University, Kumamoto, Japan

ARTICLE INFO

Article history:
Received 24 July 2012
Available online 1 August 2012

Keywords:
Diabetes mellitus
HNF1α
Transcription factor
Pancreatic β-cell
HGF

ABSTRACT

HNF1α is a transcription factor that is expressed in pancreatic β-cells and mutations of the HNF1α gene cause a form of monogenic diabetes. To understand the role of HNF1α in pancreatic β-cells, we established the MIN6 β-cell line that stably expressed HNF1α-specific shRNA. Expression of the gene encoding hepatocyte growth factor (HGF) activator (Hgfac), a serine protease that efficiently activates HGF, was decreased in HNF1α KD-MIN6 cells. Down-regulation of *Hgfac* expression was also found in the islets of HNF1α (+/−) mice. Reporter gene analysis and the chromatin immunoprecipitation assay indicated that HNF1α directly regulates the expression of *Hgfac* in β-cells. It has been reported that HGF has an important influence on β-cell mass and β-cell function. Thus, HNF1α might regulate β-cell mass or function at least partly by modulating Hgfac expression.

1. Introduction

HNF1α is a transcription factor that belongs to a subclass of the homeodomain family, and it is expressed in the liver, pancreas, kidney, and intestine [1,2]. HNF1α has an N-terminal dimerization domain, a DNA-binding domain with POU-like and homeodomain-like motifs, and a C-terminal transactivation domain [3]. We previously reported that heterozygous mutations of the HNF1α gene cause a form of monogenic diabetes known as maturity-onset diabetes of the young type 3 (MODY3) [4]. Clinical studies have shown that the primary cause of MODY3 is impairment of insulin secretion in response to a glucose load [5]. Mutant mice with loss of HNF1α function also develop diabetes due to impaired insulin secretion [6,7], indicating an important role of HNF1α in pancreatic β-cells. Interestingly, these mutant mice exhibit progressive reduction of β-cell numbers, suggesting that some target genes of HNF1α are also required for the maintenance of a normal β-cell mass.

To better understand the role of HNF1α in pancreatic β-cells and in the molecular mechanisms of MODY3, identification of the full spectrum of genes regulated by this factor in β-cells is necessary. Previous studies have demonstrated that *Slc2a2* (encoding glucose transporter 2 (GLUT2)), *Pklr* (encoding liver pyruvate kinase), *Tmem27* (encoding collectrin), *Hnf4a* (encoding HNF4α), and *Foxa3* (encoding HNF3γ) are direct targets of HNF1α in β-cells [8–12]. Genome-wide expression profiling has also been performed to identify additional targets of HNF1α using pancreatic islets obtained from control and HNF1α (−/−) knockout (KO) mice [13]. Although this approach revealed that expression of 5.6% of all genes was down-regulated in HNF1α KO islets, these changes might have been secondary to the onset of hyperglycemia or other effects of the diabetic state in HNF1α KO mice.

To identify the direct target genes of HNF1α in β-cells by another approach, we established the MIN6 β-cell line that stably expressed HNF1α-specific shRNA (HNF1α KD-MIN6 cells) and then compared the gene expression profile between control MIN6 cells and HNF1α KD-MIN6 cells. As a result, we demonstrated the down-regulation of several genes, including *Slc2a2*, *Tmeme27*, and *Hnf4a*, in HNF1α KD-MIN6 cells. We also found that expression of the gene encoding hepatocyte growth factor (HGF) activator (Hgfac), a serine protease that efficiently activates HGF [14], was decreased in HNF1α KD-MIN6 cells. Down-regulation of *Hgfac* expression was also found in the islets of HNF1α (+/−) mice. Reporter gene analysis and the chromatin immunoprecipitation assay confirmed that HNF1α directly regulates the expression of *Hgfac* in β-cells.

* Corresponding author. Address: Department of Medical Biochemistry, Faculty of Life Sciences, Kumamoto University, 1-1-1 Honjo, Kumamoto, Kumamoto 860-8556, Japan. Fax: +81 96 364 6940.
E-mail address: k-yamaga@kumamoto-u.ac.jp (K. Yamagata).

0006-291X/$ - see front matter © 2012 Elsevier Inc. All rights reserved.
http://dx.doi.org/10.1016/j.bbrc.2012.07.134

2. Material and methods

2.1. Cell culture

The MIN6 pancreatic β-cell line was maintained in Dulbecco's modified Eagles' medium (DMEM) (25 mM glucose) containing 10% (v/v) fetal bovine serum, 50 μM β-mercaptoethanol (β-ME), 50 U/ml penicillin, and 50 μg/ml streptomycin at 37 °C under 5% CO_2 [15]. Hela cells and Plat-E retrovirus packaging cells [16] were maintained in DMEM containing 10% (v/v) fetal bovine serum.

2.2. Retroviral infection

A specific shRNA sequence for mouse HNF1α (5′-CGAAGATGGTCAAGTCGTA-3′) was designed using the Clontech RNAi target sequence (http://bioinfo.clontech.com/). Oligonucleotides encoding shRNA were synthesized and cloned into the pSIREN-RetroQ retroviral shRNA expression vector (Clontech/Takara, Japan). Then the pSIREN-RetroQ-HNF1α vector and the negative control pSIREN-RetroQ vector were transfected into Plat-E cells using FuGENE6 (Roch, Germany). MIN6 cells were infected with either retrovirus and then selected by incubation with puromycin (5 μg/ml) to generate MIN6 cells stably expressing HNF1α shRNA (HNF1α KD-MIN6 cells) or negative control shRNA (control MIN6 cells), as described previously [17].

2.3. Quantitative RT-PCR

Total RNA was extracted by using Sepasol RNA I super reagent (Nacalai Tesque, Japan) or an RNeasy micro kit (Qiagen, CA). Quantitative real-time PCR was performed with SYBR Premix Ex Taq II (RR820A, TaKaRa) in an ABI 7300 thermal cycler (Applied Biosystems, CA). The specific primers were as follows: *Hnf1α* (5′-AAGAGCCCACAGGCGATGAG-3′ and 5′-TGGATGCACTCCGCCCTATT-3′), *Hgfac* (5′-GCACCTGCCACCTGATTGTG-3′ and 5′-GCCACGCCTCG GTACTCTGT-3′), *Slc2a2* (5′-CGTCCTACGGCTCTGGCACT-3′ and 5′-CACCCCAGCGAAGAGGAAGA-3′), *Tmem27* (5′-ATTCGGTGTGATATT TTGCATTGT-3′ and 5′-TCCAGGTGGTCCTTTGTTGTT-3′), and TATA-binding protein (*Tbp*) (5′-CCCCTTGTACCCTTCACCAAT-3′ and 5′-GAAGCTGCGGTACAATTCCAG-3′). Relative expression of each gene was normalized for that of *Tbp*.

2.4. Western blotting

Cells were lysed in RIPA buffer (50 mM Tris–HCl (pH 8.0), 150 mM NaCl, 0.1% SDS, 1% NP-40, 5 mM EDTA, 0.5% sodium deoxycholate), and 1/100 (v/v) protease inhibitor cocktail (Nacalai Tesque). Total protein was separated by SDS polyacrylamide gel electrophoresis and transferred to a polyvinylidene fluoride (PVDF) membrane (ImmobilonP; Millipore, MA), which was probed with the primary antibodies. After incubation with the secondary antibodies, proteins were visualized using Chemi-Lumi One Super (Nacalai Tesque) and a LAS-1000 imaging system (Fuji Film, Japan). The primary antibodies used in this study were anti-HNF1α (1:1000) (610902; Becton, Dickinson and Company, NJ) and anti-β-actin (1:5000) (A5441; Sigma–Aldrich, MO).

2.5. Insulin secretion

After reaching 80% confluence, MIN6 cells were plated in 24-well plates at a density of 3×10^5 cells per well. After culture for 72 h, cells were preincubated at 37 °C for 60 min in Hepes–Krebs buffer (118.4 mM NaCl, 4.7 mM KCl, 1.2 mM KH_2PO_4, 2.4 mM $CaCl_2$, 1.2 mM $MgSO_4$, 20 mM $NaHCO_3$, 2.2 mM glucose, and 10 mM Hepes) containing 0.5% (w/v) bovine serum albumin (BSA) [17]. Then the cells were incubated for 60 min in Hepes–Krebs buffer containing 22 mM glucose and insulin production was measured by using a mouse insulin ELISA kit (AKRIN-011T; Shibayagi, Japan).

2.6. Microarray analysis

Total RNA was extracted from control MIN6 cells and HNF1α KD-MIN6 cells using a miRCURY RNA isolation kit (Exiqon, Denmark) according to the manufacturer's instructions. The quality of the RNA was checked by gel electrophoresis and analysis with an Agilent 2100 Bioanalyzer (Agilent Technologies, CA). DNA microarray analysis was performed by the Toray Custom Analysis Service using the 3D-Gene™ DNA chip (Mouse Oligo chip 24K).

2.7. Isolation of pancreatic islets

HNF1α knockout mice were generated that lacked exon 1, which contains the translation start codon [K. Yamamura, and K. Yamagata, unpublished data]. HNF1α (+/−) mice showed normal glucose tolerance, as reported previously [6, and our unpublished data]. Mice were maintained with a 12 h light–12 h dark cycle and were allowed free access to food and water. These experiments were conducted according to the guidelines of the Institutional Animal Committee of Kumamoto University. Islets were isolated from the harvested pancreata of 20-week-old male HNF1α (+/−) mice ($n = 4$) and control HNF1α (+/+) littermates ($n = 4$) by collagenase digestion, as described previously [7].

2.8. Transient transfection and luciferase reporter assay

A 135 bp fragment of the mouse Hgfac gene promoter containing the putative HNF1α-binding site (−135 to −1 relative to the translation start codon when A is numbered as +1) was amplified by PCR using the primers 5′-GCTAGCGGCTGTGGAGGAGCCTAACAGGAT-3′ (underlined nucleotides indicate the cloned NheI site) and 5′-AAGCTTGGCTCCTCCTGAGCTGGCGTGAGG-3′ (underlined nucleotides indicate the cloned HindIII site), and then was subcloned into the pGL3 basic reporter (Promega, WI) to generate pGL3-Hgfac. The HNF1α-binding site was altered to 5′-GGTCGGCCCTTATCA-3′ by PCR-based mutagenesis. The pcDNA3.1-wild-type (WT)-HNF1α and pcDNA3.1-P291fsinsC-HNF1α expression plasmids have been described previously [8]. Hela cells (1.5×10^5 cells/well) or MIN6 cells (3×10^5 cells/well) were seeded into 12-well plates at 18 h before transient transfection was performed using X-treme GENE (Roche) according to the manufacturer's instructions. At 48 h after transfection, luciferase activity was measured by using a Dual-Luciferase Reporter assay system (Promega).

2.9. Chromatin immunoprecipitation (ChIP) assay

MIN6 cells were cross-linked with 1% formaldehyde for 10 min at room temperature. Then the ChIP assay was performed as described previously [17] using an anti-HNF1 antibody (sc-8986, Santa Cruz Biotechnology, CA). Immunoprecipitated DNA was amplified by real-time PCR with specific primers for the promoter region of *Hgfac* containing the HNF1α-binding motif (5′-GGCTGTG GAGGAGCCTAACAGGAT-3′ and 5′-GGCTCCTCCTGAGCTGGCGT-GAGG-3′) (P1), as well as primers for the 10 kb upstream region from the *Hgfac* translation start codon (5′-GGGCTGGGGT GC TTCGGGTA-3′ and 5′-GACCCTCCAGCGGATGGC TCA-3′) (P2), the 5.3 kb downstream region from the *Hgfac* translation start (5′-GCTGTGCTGTCCGCTCCCAG-3′ and 5′-CATGTGGCCCCAGCCTGCAA-3′) (P3), and the promoter region of *Tbp* (5′-ATCAGATGTGCGT-CAGGCGTT-3′ and 5′-TGCGGAGAAAATGACGCGA-3′) (P4). All PCR

reactions were done by using SYBR Premix Ex Taq II (TaKaRa) in an ABI 7300 thermal cycler (Applied Biosystems).

2.10. Statistical analysis

The significance of differences was assessed with the unpaired *t*-test, and $p < 0.05$ was considered to indicate statistical significance.

3. Results

3.1. Establishment of HNF1α KD-MIN6 cells and microarray analysis

In order to identify novel target genes for HNF1α in pancreatic β-cells, we established MIN6 β-cells that stably expressed HNF1α-specific shRNA (HNF1α KD-MIN6) by retroviral infection. Suppression of endogenous HNF1α expression by shRNA was confirmed at both the mRNA level (39.8% of control, $p = 0.019$) and the protein level (30.6% of control, $p = 0.007$) (Fig. 1A and B). *Slc2a2* and *Tmem27* are direct targets of HNF1α in β-cells [10,11], and expression of both these genes was significantly decreased in HNF1α KD-MIN6 cells (Fig. 1C). Loss of the function of HNF1α leads to impairment of glucose-stimulated insulin secretion by pancreatic β-cells [6,7]. Therefore, we examined insulin secretion by HNF1α KD-MIN6 cells and control MIN6 cells. Insulin secretion by HNF1α KD-MIN6 cells subjected to stimulation with 22 mM glucose was significantly decreased ($p < 0.001$) to 39.2% of that for control cells (Fig. 1D). Suppression of HNF1α expression also reduced insulin secretion by HNF1α KD-MIN6 cells in response to a low glucose concentration (decreased by 41.4%, $p < 0.001$). These results indicate that HNF1α KD-MIN6 cells can be used as a novel cellular model of MODY3.

In order to identify novel target genes of HNF1α in pancreatic β-cells, DNA microarray analysis was performed using control cells and HNF1α KD-MIN6 cells. Microarray analysis identified the down-regulation of 53 genes (0.22% of all expressed genes), which was defined as a signal log ratio $\leqslant -1.5$, in HNF1α KD-MIN6 cells and up-regulation of 38 genes (0.15% of all expressed genes), which was defined as a signal log ratio $\geqslant 2$ (Table 1 and Supplementary Table 1). Several known targets of HNF1α (*Slc2a2*, *Tmem27*, and *Hnf4α* were found in the group of down-regulated genes.

3.2. Hgfac expression in β-cells is regulated by HNF1α

Microarray analysis revealed that expression of the gene encoding hepatocyte growth factor activator (HGFA) was reduced to 25.2% of the control level in HNF1α KD-MIN6 cells (Table 1). Down-regulation of *Hgfac* expression in HNF1α KD-MIN6 cells to 18.7% of the control level ($p < 0.001$) was confirmed by quantitative RT-PCR (Fig. 2A). HNF1α (+/−) mice were reported to be useful for investigating HNF1α-dependent transcription in pancreatic islets [18]. As shown in Fig. 2B, Hgfac mRNA expression was significantly decreased in the islets of HNF1α (+/−) mice to 45.8% of the control level ($p < 0.001$), indicating that *Hgfac* gene transcription is regulated by HNF1α *in vivo* as well as *in vitro*.

Screening of the promoter region of the mouse *Hgfac* gene by using a genomic databank revealed an HNF1α-binding site (nucleotides −83 to −97 relative to the translation start codon when *A* is designated as +1), and this binding site was also confirmed to exist in the human HGFAC gene (Fig. 2C). We cloned a 135 bp fragment

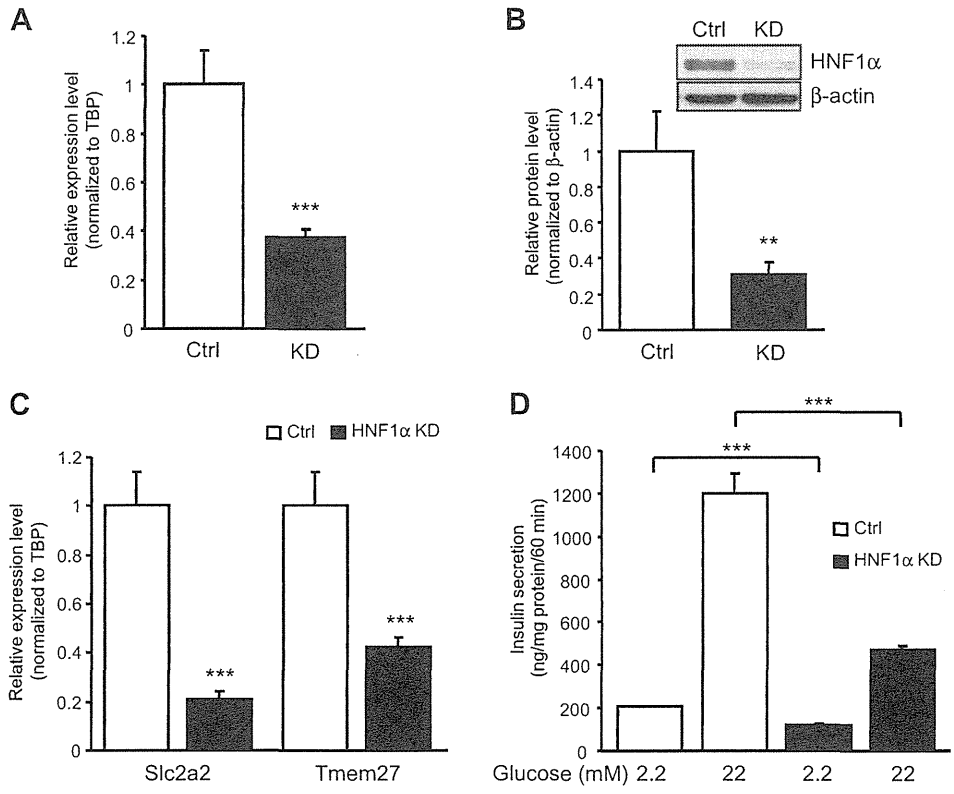

Fig. 1. Gene expression and insulin secretion by HNF1α KD-MIN6 cells. (A) Expression of HNF1α mRNA by control cells (Ctrl) ($n = 3$) and HNF1α KD-MIN6 cells (KD) ($n = 3$). Expression is normalized for that of Tbp. (B) HNF1α protein expression in HNF1α KD-MIN6 cells evaluated by Western blotting ($n = 3$). β-actin was used as the loading control. (C) Expression of Slc2a2 and Tmem27 mRNA was significantly decreased in HNF1α KD-MIN6 cells ($n = 3$). (D) Insulin secretion after exposure to glucose was decreased in HNF1α KD-MIN6 cells ($n = 4$). Data are the mean ± SD (**$p < 0.01$, ***$p < 0.001$).

Table 1
Gene list of the down-regulated genes in HNF1α KD-MIN6 cells.

Gene symbol	Gene title	Log ratio	RefSeq transcript ID
Gc	Group specific component	−3.76	NM_008096
Ugt1a6a	UDP glucuronosyltransferase 1 family, polypeptide A7C	−3.68	NM_145079
Slc2a2	Solute carrier family 2 (facilitated glucose transporter), member 2	−3.61	NM_031197
Crp	C-reactive protein, pentraxin-related	−3.48	NM_007768
Ttr	Transthyretin	−3.23	NM_013697
Tmed6	Transmembrane emp24 protein transport domain containing 6	−3.02	NM_025458
Serpina1c	Serine (or cysteine) peptidase inhibitor, clade A, member 1a	−2.90	NM_009245
Iyd	Iodotyrosine deiodinase	−2.80	NM_027391
Slc40a1	Solute carrier family 40 (iron-regulated transporter), member 1	−2.70	NM_016917
Ang1	Angiogenin, ribonuclease A family, member 1	−2.70	NM_007447
Spon2	Spondin 2, extracellular matrix protein	−2.64	NM_133903
Rnase4	Ribonuclease, RNase A family 4	−2.62	NM_021472
Golt1a	Golgi transport 1 homolog A (S. cerevisiae)	−2.53	NM_026680
Serpina1c	Serine (or cysteine) peptidase inhibitor, clade A, member 1a	−2.50	NM_009243
Serpina1d	Serine (or cysteine) peptidase inhibitor, clade A, member 1d	−2.44	NM_009246
Serpina1e	Serine (or cysteine) peptidase inhibitor, clade A, member 1e	−2.33	NM_009247
Guca1a	Guanylate cyclase activator 1a (retina)	−2.29	NM_008189
Nmbr	Neuromedin B receptor	−2.29	NM_008703
Tmem27	Transmembrane protein 27	−2.26	NM_020626
Ang4	Angiogenin, ribonuclease A family, member 4	−2.24	NM_177544
Ang5	Angiogenin, ribonuclease A family, member 5	−2.21	NM_007448
Dpp4	Dipeptidylpeptidase 4	−2.20	NM_010074
Ldha	Lactate dehydrogenase A	−2.11	NM_010699
St6gal1	Beta galactoside alpha 2,6 sialyltransferase 1	−2.05	NM_145933
Hgfac	Hepatocyte growth factor activator	−1.99	NM_019447
Pcsk9	Proprotein convertase subtilisin/kexin type 9	−1.98	NM_153565
Ang5	Angiogenin, ribonuclease A family, member 5	−1.97	NM_007448
Abcg2	ATP-binding cassette, sub-family G (WHITE), member 2	−1.96	NM_011920
Ins1	Insulin I	−1.92	NM_008386
Kif12	Kinesin family member 12	−1.89	NM_010616
Ppp1r1a	Protein phosphatase 1, regulatory (inhibitor) subunit 1A	−1.87	NM_021391
Itga6	Integrin alpha 6	−1.84	NM_008397
Myo15b	Myosin XVB	−1.84	XM_203357
Il20rb	Interleukin 20 receptor beta	−1.83	XM_358706
Degs2	Degenerative spermatocyte homolog 2 (Drosophila), lipid desaturase	−1.81	NM_027299
Tff3	Trefoil factor 3, intestinal	−1.75	NM_011575
Cpn1	Carboxypeptidase N, polypeptide 1	−1.71	NM_030703
Cbs	Cystathionine beta-synthase	−1.71	NM_144855
Insl5	Insulin-like 5	−1.70	NM_011831
Slc16a3	Solute carrier family 16 (monocarboxylic acid transporters), member 3	−1.70	NM_030696
Mbl2	Mannose binding lectin (protein C)	−1.68	NM_010776
Tm4sf4	Transmembrane 4 superfamily member 4	−1.67	NM_145539
Dact2	Dapper homolog 2, antagonist of beta-catenin (xenopus)	−1.63	NM_172826
Dscr1l1	Down syndrome critical region gene 1-like 1	−1.63	NM_030598
Anks4b	Ankyrin repeat and sterile alpha motif domain containing 4B	−1.61	NM_028085
Cacna1 h	Calcium channel, voltage-dependent, T type, alpha 1H subunit	−1.60	NM_021415
Il6ra	Interleukin 6 receptor, alpha	−1.59	NM_010559
Hnf4a	Hepatic nuclear factor 4, alpha	−1.59	NM_008261
Defb1	Defensin beta 1	−1.58	NM_007843
Sgk2	Serum/glucocorticoid regulated kinase 2	−1.56	NM_013731
Sct	Secretin	−1.52	NM_011328
Lgals2	Lectin, galactose-binding, soluble 2	−1.52	NM_025622
Nek6	NIMA (never in mitosis gene a)-related expressed kinase 6	−1.51	NM_021606

of the promoter region upstream of a luciferase reporter gene, and co-expressed it with the HNF1α expression vector in HeLa cells. We found that induction of HNF1α increased *Hgfac* promoter activity to 23.6 times the control level ($p < 0.001$) (Fig. 2D). HNF1α also activated the reporter gene by 3.1-fold ($p < 0.001$) in MIN6 cells, while dominant negative P291fsinsC-HNF1α (a frameshift mutation in the transactivation domain) [8] decreased reporter gene activity to 41.0% of the control level ($p < 0.001$) (Fig. 2E). Mutation of the putative HNF1α-binding site in the reporter gene significantly reduced transcriptional activation by HNF1α (87.3% decrease, $p < 0.001$) (Fig. 2F).

In order to investigate binding of HNF1α to the Hgfac promoter, the chromatin immunoprecipitation (ChIP) assay was performed. Cross-linked chromatin was precipitated with HNF1 antibody, after which the precipitated DNA was analyzed by PCR using primer sets that amplified the promoter region of *Hgfac* containing the putative HNF1α-binding site (P1), the 10 kb upstream region from P1 (P2), the 5.3 kb downstream region from P1 (exon 12) (P3), and the promoter region of *Tbp* (P4). As shown in Fig. 2G, specific binding of HNF1α to the promoter region (P1) was identified in MIN6 cells. These findings indicated that the *Hgfac* gene is directly regulated by HNF1α.

4. Discussion

HGF was originally identified as a potent mitogen for hepatocytes [19], but subsequent studies have shown that it has mitogenic and prosurvival effects on various cells including β-cells. Transgenic overexpression of HGF in pancreatic β-cells increases β-cell replication, mass, and function [20]. Loss of HGF signaling in β-cells during gestation leads to decreased replication and a

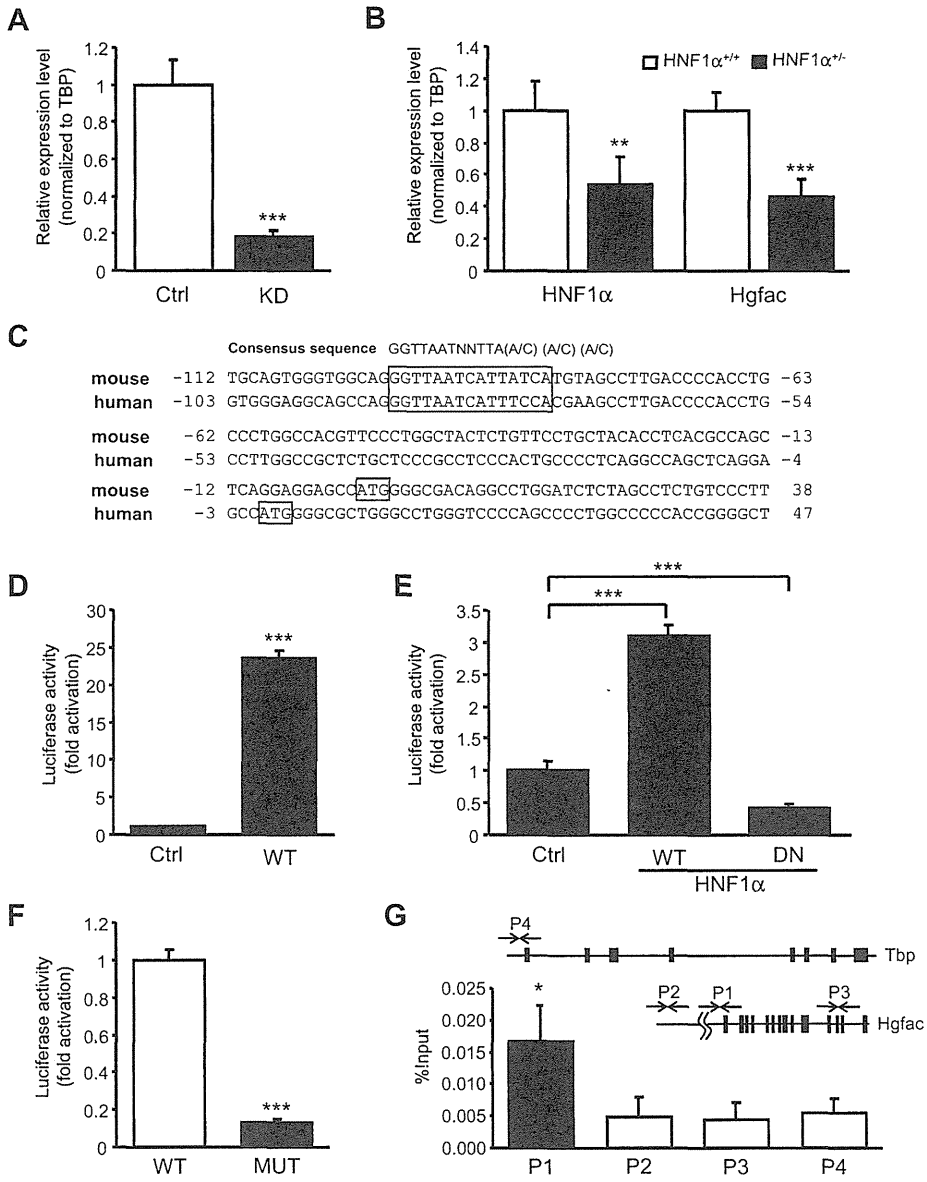

Fig. 2. Transcriptional regulation of *Hgfac* by HNF1α. (A) Expression of Hgfac mRNA by control (Ctrl) cells ($n = 3$) and HNF1α KD-MIN6 cells (KD) ($n = 3$). Expression is normalized for that of Tbp. (B) Expression of HNF1α and Hgfac mRNA in HNF1α (+/+) ($n = 4$) and HNF1α (+/−) islets ($n = 4$). (C) DNA sequences of the mouse and human Hgfac genes. The putative HNF1α-binding site is shown by a box. (D) HeLa cells were cotransfected with 800 ng of the pcDNA3.1-HNF1α expression vector as well as 200 ng of the pGL3-Hgfac reporter vector and 1 ng of pRL-TK. (E) MIN6 cells were cotransfected with 800 ng of the pcDNA3.1-HNF1α (WT) or the pcDNA3.1-P291fsinsC-HNF1α (DN) expression vector as well as 200 ng of the pGL3-Hgfac reporter vector and 0.4 ng of pRL-TK. (F) MIN6 cells were cotransfected with 800 ng of the pcDNA3.1-HNF1α (WT) expression vector as well as 200 ng of the pGL3-Hgfac (WT) or pGL3-Hgfac-mutant (MUT) reporter vector and 0.4 ng of pRL-TK. (G) Chromatin immunoprecipitation assay with MIN6 cells. PCR was performed using 4 different primer sets (P1–P4). The P2–4 regions lack the HNF1α-binding motif. Interaction of HNF1α with the P1 region of *Hgfac* was observed. Data are the mean ± SD (*$p < 0.05$, **$p < 0.01$, ***$p < 0.001$).

decline of β-cell mass, and loss of HGF signaling also accelerates the onset of diabetes in response to multiple low-dose injections of streptozotocin [21,22]. These data strongly suggest that HGF has an important influence on β-cell mass and β-cell function.

HGF is secreted in a latent form, and proteolytic conversion by the serine protease HGF activator (Hgfac) is required for its activation [14]. In this study, we found that Hgfac expression was markedly decreased in both HNF1α KD-MIN6 cells and islets from HNF1α (+/−) mice. The reporter and ChIP assays demonstrated that HNF1α bound to the conserved binding site of the *Hgfac* promoter and that it activated transcription of this gene, indicating that *Hgfac* is a direct target of HNF1α in β-cells. Although the molecular mechanisms underlying MODY3 are still unknown, HNF1α (−/−) mice and transgenic mice expressing the naturally occurring dominant negative form of human HNF1α (P291fsinsC) in their β-cells exhibit progressive reduction of β-cell mass and β-cell proliferation, indicating that HNF1α is required to maintain the β-cell mass [6,7]. Reduction of *Hgfac* gene expression and a consequent decrease of HGF signaling in β-cells might occur in HNF1α mutant mice as well as in patients with MODY3. It is possible that HNF1α controls β-cells mass at least partly by regulating cellular Hgfac expression. Investigation of β-cell specific Hgfac knockout mice could improve our understanding of how a reduction of HNF1α activity leads to a decline of β-cell mass and the onset of diabetes.

In conclusion, we established a novel cellular model of MODY3, HNF1α KD-MIN6 cells, and we identified many genes that were down-regulated in these cells. Further investigation of HNF1α KD-MIN6 cells could be useful to identify novel target genes of HNF1α in β-cells.

Acknowledgments

We thank Prof. Miyazaki (Osaka University) for the kind gift of MIN6 cells, and Prof. T. Kitamura (Tokyo University) for providing Plat-E cells. This work was supported by a Grant-in-Aid for Scientific Research (S), a Grant-in-Aid for Scientific Research on Innovative Areas, Health Labour Sciences Research Grant, and Grants from the Takeda Science Foundation, Novo Nordisk Insulin Research Foundation, Banyu Life Science Foundation International, and Japan Diabetes Foundation.

Appendix A. Supplementary data

Supplementary data associated with this article can be found, in the online version, at http://dx.doi.org/10.1016/j.bbrc.2012.07.134.

References

[1] D.B. Mendel, G.R. Crabtree, HNF-1, a member of a novel class of dimerizing homeodomain proteins, J. Biol. Chem. 266 (1991) 677–680.
[2] T. Nammo, K. Yamagata, R. Hamaoka, Q. Zhu, T. Akiyama, F. Gonzalez, J. Miyagawa, Y. Matsuzawa, Expression profile of MODY3/HNF-1α protein in the developing mouse pancreas, Diabetologia 45 (2002) 1142–1153.
[3] M. Frain, G. Swart, P. Monaci, A. Nicosia, S. Stilmpfli, R. Frank, R. Cortese, The liver-specific transcription factor LF-B1 contains a highly diverged homeobox DNA binding domain, Cell 59 (1989) 145–157.
[4] K. Yamagata, N. Oda, P.J. Kaisaki, S. Menzel, H. Furuta, M. Vaxillaire, L. Southam, R.D. Cox, G.M. Lathrop, V.V. Boriraj, X. Chen, N.J. Cox, Y. Oda, H. Yano, M.M. Le Beau, S. Yamada, H. Nishigori, J. Takeda, S.S. Fajans, A.T. Hattersleystar, N. Iwasaki, T. Hansen, O. Pedersen, K.S. Polonsky, R.C. Turner, G. Velho, J-C. Chèvreparallel, P. Froguel, G.I. Bell, Mutations in the hepatocyte nuclear factor-1α gene in maturity-onset diabetes of the young (MODY3), Nature 384 (1996) 455–458.
[5] M.M. Byrne, J. Sturis, S. Menzel, K. Yamagata, S.S. Fajans, M.J. Dronsfield, S.C. Bain, A.T. Hattersley, G. Velho, P. Froguel, G.I. Bell, K.S. Polonsky, Altered insulin secretory responses to glucose in diabetic and nondiabetic subjects with mutations in the diabetes susceptibility gene MODY3 on chromosome 12, Diabetes 45 (1996) 1503–1510.
[6] M. Pontoglio, S. Sreenan, M. Roe, W. Pugh, D. Ostrega, A. Doyen, A.J. Pick, A. Baldwin, G. Velho, P. Froguel, M. Levisetti, S. Bonner-Weir, G.I. Bell, M. Yaniv, K.S. Polonsky, Defective insulin secretion in hepatocyte nuclear factor 1α-deficient mice, J. Clin. Invest. 101 (1998) 2215–2222.
[7] K. Yamagata, T. Nammo, M. Moriwaki, A. Ihara, K. Iizuka, Q. Yang, T. Satoh, M. Li, R. Uenaka, K. Okita, H. Iwahashi, Q. Zhu, Y. Cao, A. Imagawa, Y. Tochino, T. Hanafusa, J. Miyagawa, Y. Matsuzawa, Mutant hepatocyte nuclear factor-1α in pancreatic β-cells causes abnormal islet architecture with decreased expression of E-cadherin, reduced β-cell proliferation, and diabetes, Diabetes 51 (2002) 114–123.
[8] K. Yamagata, Q. Yang, K. Yamamoto, H. Iwahashi, J. Miyagawa, K. Okita, I. Yoshiuchi, J. Miyazaki, T. Noguchi, H. Nakajima, M. Namba, T. Hanafusa, Y. Matsuzawa, Mutation P291fsinsC in the transcription factor hepatocyte nuclear factor-1α is dominant negative, Diabetes 47 (1998) 1231–1235.
[9] H. Wang, P. Maechler, K.A. Hagenfeldt, C.B. Wollheim, Dominant-negative suppression of HNF-1α function results in defective insulin gene transcription and impaired metabolism-secretion coupling in a pancreatic β-cell line, EMBO J. 17 (1998) 6701–6713.
[10] S.F. Boj, M. Parrizas, M.A. Maestro, J. Ferrer, A transcription factor regulatory circuit in differentiated pancreatic cells, Proc. Natl. Acad. Sci. USA 98 (2001) 14481–14486.
[11] K. Fukui, Q. Yang, Y. Cao, N. Takahashi, H.H. Atakeyama, H. Wang, J. Wada, Y. Zhang, L. Marselli, T. Nammo, K. Yoneda, M. Onishi, S. Higashiyama, Y. Matsuzawa, F.J. Gonzalez, G.C. Weir, H. Kasai, I. Shimomura, J. Miyagawa, C.B. Wollheim, K. Yamagata, The HNF-1 target collectrin controls insulin exocytosis by SNARE complex formation, Cell Metab. 2 (2005) 373–384.
[12] P. Akpinar, S. Kuwajima, J. Krützfeldt, M. Stoffel, Tmem27: a cleaved and shed plasma membrane protein that stimulates pancreatic beta cell proliferation, Cell Metab. 2 (2005) 385–397.
[13] J.M. Servitja, M. Pignatelli, M.A. Maestro, C. Cardalda, S.F. Boj, J. Lozano, E. Blanco, A. Lafuente, M.I. McCarthy, L. Sumoy, R. Guigó, J. Ferrer, Hnf1α (MODY3) controls tissue-specific transcriptional programs and exerts opposed effects on cell growth in pancreatic islets and liver, Mol. Cell Biol. 29 (2009) 2945–2959.
[14] K. Miyazawa, Hepatocyte growth factor activator (HGFA): a serine protease that links tissue injury to activation of hepatocyte growth factor, FEBS J. 277 (2010) 2208–2214.
[15] J. Miyazaki, K. Araki, E. Yamato, H. Ikegami, T. Asano, Y. Shibasaki, Y. Oka, K. Yamamura, Establishment of a pancreatic beta cell line that retains glucose-inducible insulin secretion: special reference to expression of glucose transporter isoforms, Endocrinology 127 (1990) 126–132.
[16] T. Kitamura, Y. Koshino, F. Shibata, T. Oki, H. Nakajima, T. Nosaka, H. Kumagai, Retrovirus-mediated gene transfer and expression cloning: powerful tools in functional genomics, Exp. Hematol. 31 (2003) 1007–1014.
[17] Y. Sato, M. Hatta, M.F. Karim, T. Sawa, F.Y. Wei, S. Sato, M.A. Magnuson, F.J. Gonzalez, K. Tomizawa, T. Akaike, T. Yoshizawa, K. Yamagata, Anks4b, a novel target of HNF4α protein interacts with GRP78 protein and regulates endoplasmic reticulum stress-induced apoptosis in pancreatic β-cells, J. Biol. Chem. 287 (2012) 23236–23245.
[18] S.F. Boj, D. Petrov, J. Ferrer, Epistasis of transcriptomes reveals synergism between transcriptional activators Hnf1α and Hnf4α, PLoS Genetics 6 (2010) e1000970.
[19] T. Nakamura, T. Nishizawa, M. Hagiya, T. Seki, M. Shimonishi, A. Sugimura, K. Tashiro, S. Shimizu, Molecular cloning and expression of human hepatocyte growth factor, Nature 342 (1989) 440–443.
[20] A. Garcia-Ocaña, K.K. Takane, M.A. Syed, W.M. Philbrick, R.C. Vasavada, A.F. Stewart, Hepatocyte growth factor overexpression in the islet of transgenic mice increases beta cell proliferation, enhances islet mass, and induces mild hypoglycemia, J. Biol. Chem. 275 (2000) 1226–1232.
[21] J. Mellado-Gil, T.C. Rosa, C. Demirci, J.A. Gonzalez-Pertusa, S. Velazquez-Garcia, S. Ernst, S. Valle, R.C. Vasavada, A.F. Stewart, L.C. Alonso, A. Garcia-Ocan~a, Disruption of hepatocyte growth factor/c-Met signaling enhances pancreatic beta-cell death and accelerates the onset of diabetes, Diabetes 60 (2011) 525–536.
[22] C. Demirci, S. Ernst, J.C. Alvarez-Perez, T. Rosa, S. Valle, V. Shridhar, G.P. Casinelli, L.C. Alonso, R.C. Vasavada, A. García-Ocana, Loss of HGF/c-Met signaling in pancreatic β-cells leads to incomplete maternal β-cell adaptation and gestational diabetes mellitus, Diabetes 61 (2012) 1143–1152.

Original Article

Augmentation of Smad-dependent BMP signaling in neural crest cells causes craniosynostosis in mice†

Yoshihiro Komatsu[1,2], Paul B. Yu[3], Nobuhiro Kamiya[1,2,4], Haichun Pan[1], Tomokazu Fukuda[2,5], Gregory J. Scott[6], Manas K. Ray[6], Ken-ichi Yamamura[7], Yuji Mishina[1,2,6]

[1]Department of Biologic and Materials Sciences, School of Dentistry, University of Michigan, Ann Arbor, MI 48109, USA, [2]Laboratory of Reproductive and Developmental Toxicology, National Institute of Environmental Health Sciences, National Institutes of Health, Research Triangle Park, NC 27709, USA, [3]Division of Cardiology, Department of Medicine, Massachusetts General Hospital and Harvard Medical School, Thier 505, 50 Blossom Street, Boston, MA 02114, USA, [4]Center for Excellence in Hip Disorders, Texas Scottish Rite Hospital for Children, Dallas, TX 75219, USA, [5]Graduate School of Agricultural Science, Tohoku University, Sendai 981-8555, Japan, [6]Knock Out Core, National Institute of Environmental Health Sciences, National Institutes of Health, Research Triangle Park, NC 27709, USA, [7]Institute of Molecular Embryology and Genetics, Kumamoto University, Kumamoto 860-0811, Japan.

Corresponding author: Yuji Mishina, Ph.D.
Department of Biologic and Materials Sciences
School of Dentistry, University of Michigan
1011 N. University Ave., Ann Arbor, MI 48109, USA.
Tel: +1-734-763-5579, Fax: +1-734-647-2110, Email: mishina@umich.edu

Additional Supporting Information may be found in the online version of this article.

Initial Date Submitted July 19, 2012; Date Revision Submitted November 19, 2012; Date Final Disposition Set December 5, 2012

Journal of Bone and Mineral Research

DOI 10.1002/jbmr.1857

Abstract

Craniosynostosis describes conditions in which one or more sutures of the infant skull are prematurely fused, resulting in facial deformity and delayed brain development. Approximately 20% of human craniosynostoses are thought to result from gene mutations altering growth factor signaling; however, the molecular mechanisms by which these mutations cause craniosynostosis are incompletely characterized, and the causative genes for diverse types of syndromic craniosynostosis have yet to be identified. Here, we show that enhanced bone morphogenetic protein (BMP) signaling through the BMP type IA receptor (BMPR1A) in cranial neural crest cells, but not in osteoblasts, causes premature suture fusion in mice. In support of a requirement for precisely regulated BMP signaling, this defect was rescued on a *Bmpr1a* haploinsufficient background, with corresponding normalization of Smad phosphorylation. Moreover, in vivo treatment with LDN-193189, a selective chemical inhibitor of BMP type I receptor kinases resulted in partial rescue of craniosynostosis. Enhanced signaling of the fibroblast growth factor (FGF) pathway, which has been implicated in craniosynostosis, was observed in both mutant and rescued mice, suggesting that augmentation of FGF signaling is not the sole cause of premature fusion found in this model. The finding that relatively modest augmentation of Smad-dependent BMP signaling leads to premature cranial suture fusion suggests an important contribution of dysregulated BMP signaling to syndromic craniosynostoses, and potential strategies for early intervention.

Keywords: BMP, Craniosynostosis, Neural crest cells, Smad-signaling, Suture

Introduction

Craniosynostosis, a syndrome of premature fusion of cranial sutures, affects one in 2,500 live births (1,2). This condition results in facial deformity and restricted brain growth, with challenging clinical management that often requires multiple corrective surgeries. Individuals with craniosynostosis left untreated during infancy develop increased intracranial pressure that can cause chronic headaches and gradual loss of vision, and are at risk for cognitive impairment. Craniofacial abnormalities seen with craniosynostosis can also cause upper airway obstruction and sleep apnea (3).

Craniosynostosis is a devastating disorder, for which the only treatment is carefully timed and extensive reconstructive surgery. Although advances in molecular genetics past decades have revealed several gene mutations which can result in craniosynostosis, the molecular pathophysiology of craniosynostosis in humans remains incompletely understood. Limited cases of syndromic craniosynostoses (20-30%) have been found to be associated with the mutations of fibroblast growth factor receptor family (FGFR1, FGFR2 and FGFR3), MSX2, TWIST1 and EFNB1 in man; however, the genetic basis of most craniosynostoses have yet to be identified (1,2). Craniosynostosis has diverse presentations, which include the Apert, Boston, Crouzon, Pfeiffer, Jackson-Weiss and Saethre-Chotzen syndromes (1,2). While coronal sutures are commonly affected in these syndromes, each syndrome has a unique pattern of suture fusions. For example, the sagittal suture is frequently fused in both Crouzon and Pfeiffer syndromes but not in Saethre-Chotzen syndrome. The unique pattern of fusion in each syndrome suggests that distinct developmental processes underlie various premature suture fusion phenotypes. Defining the molecular and cellular pathogenesis of each syndromic craniosynostosis could facilitate strategies for the early identification, prevention or treatment of these developmental defects.

Bone morphogenetic proteins (BMPs) play broad roles in developmental patterning, including skull morphogenesis (4-7). Gain-of-function mutations in MSX2, a member of the homeobox gene family whose transcription is regulated by BMP and TGF-β signaling, result in an autosomal dominant Boston-type craniosynostosis in man, while mice overexpressing *Msx2* also develop premature fusion of coronal and sagittal sutures (8,9). Moreover, the endogenous BMP antagonist noggin is expressed in non-fusing sutures, and is observed to enforce suture patency in mice (10). These prior observations suggest that appropriate levels of BMP signaling may be critical for maintaining normal suture patency during skull development and that dysregulated BMP signaling may contribute to craniosynostosis.

Since the frontal region of cranial bones and sutures are derived from a distinct multipotent cell population, i.e., cranial neural crest (CNC) cells (11-13), we hypothesized that aberrant differentiation of CNC cells caused by alterations in BMP signaling results in cranial malformations. To test this hypothesis, we developed a conditional mouse model with enhanced BMP signaling in the skull and sutures. We found that failure to maintain precisely controlled Smad-dependent BMP signaling in CNC cells but not in osteoblast-committed cells led to craniosynostosis. We also found that reduction of BMP signaling by genetic or pharmacological methods rescued the premature fusion found in the metopic suture, as well as abnormalities found in CNC-derived skull bones. In this enhanced BMP signaling model, we also observed enhanced FGF ligand expression. However, these perturbations in FGF signaling did not appear to account for craniosynostosis, in contrast to the phenotypes observed in FGF gain-of-function mutant mice (14-17). These results lend novel mechanistic support for the concept that supraphysiological levels of BMP signaling contribute to some human craniosynostoses, which in turn might be mitigated by pharmacologic blockade early in their genesis.

Materials and Methods

Generation of ca-Bmpr1a mouse lines

A plasmid containing human *BMPR1A* cDNA with a Q233D mutation was kindly obtained from Dr. T. Imamura (Cancer Institute of Japan). The cDNA fragment was inserted into a *Pst*I site of the CAG-Z-EGFP vector (18,19). The transgenic vector was linearized and electroporated into AB2.2 mouse ES cells (Lexicon Genetics) with a PGKneobpA plasmid for selection with G418. Ninety-six G418 resistant colonies were stained for β-gal activity to confirm the expression of the transgene. Four of representative ES clones, which showed relatively strong expressions of β-gal activity, were injected into blastocysts from C57BL/6 mice, and 3 of them (clones A3, F1 and F2) underwent germline transmission. Progenies bred with wild-type C57BL/6 showed expected ration of transmission of the transgene (50%), indicating that transgenic mouse lines have a single integration site for transgene in its genome. We initially analyzed progenies from clone A3 and F1 to confirm that they developed identical phenotypes (Fig. S1), thus we focused transgenic line from clone A3 in the rest of analyses. *P0-Cre* mouse, C57BL/6J-Tg(P0-Cre)94Imeg (ID 148), was provided by CARD, Kumamoto University, Japan. All mouse experiments were performed in accordance with National Institute of Environmental Health Sciences and University of Michigan guidelines covering the humane care and use of animals in research.

Histology, skeletal staining, immunohistochemistry and micro-CT (μCT)

Embryos were fixed in either 10% formalin or 4% paraformaldehyde, embedded in paraffin, and stained with Hematoxylin and Eosin (H&E). Cranial bone was stained with alizarin red and alcian blue by standard methods. For immunohistochemistry, mouse skull was fixed with 4% paraformaldehyde at 4°C overnight and replaced with 20% sucrose in PBS at 4°C. Samples were embedded by O.C.T. compound and 10μm cryo-sections were cut. After

washing with PBS containing 0.1% Triton X-100, the specimens were incubated with rabbit anti-FGF2 (dilution 1:100, catalog number: AB1458, Chemicon), rabbit anti-FGFR1 (dilution 1:100, catalog number: sc-121, Santa Cruz), rabbit anti-FGFR2 (dilution 1:100, catalog number: sc-122, Santa Cruz), rabbit anti-phospho-p38 MAPK (dilution 1:50, catalog number: 4631, Cell Signaling) and rabbit anti-phospho-SMAD1/5/8 (dilution 1:100, catalog number: 9511, Cell Signaling) at 4°C overnight, with Alexa Fluor 488 donkey anti-rabbit IgG (dilution 1:100, catalog number: A21206, Invitrogen) used as secondary Ab. Sections were mounted with ProLong Gold antifade reagent with DAPI (catalog number: P36935, Invitrogen). Fluorescence images were obtained with an Olympus BX-51 microscope with an Olympus DP-70 CCD camera. Captured images were processed in Adobe Photoshop CS3 (version 10.0). Skulls were scanned using a micro-computed tomography (μCT) system at 12mm of thickness, 55kV of energy and 145mA of intensity (μCT40: Scanco Medical AG, Brüttisellen Switzerland), and reconstructed to produce 2D and 3D images (20).

Quantitative real time RT-PCR

Skull tissues were pretreated with RNA later (Ambion) and RNA isolated using TRIzol (Invitrogen). cDNA was synthesized by using SuperScript III cDNA Synthesis (Invitrogen). TaqMan probes were purchased and real time RT-PCR was performed by ABI PRISM 7500 (Applied Biosystems). Data were normalized to GAPDH by $2^{-\Delta\Delta Ct}$ method.

Establishment of preosteoblast cells from the skull

Cranial preosteoblasts were established from newborn pups as described previously (13,21). Preosteoblasts were grown in Minimum Essential Medium (alpha-MEM) (catalog number: 12561, Invitrogen) with 10% fetal bovine serum (Hyclone) and penicillin/streptomycin (catalog number: P-

0781, Sigma). 100μg/ml ascorbic acid (catalog number: A-4403, Sigma) and 4mM β-glycerophosphate (catalog number: G-9891, Sigma) were added for further primary cultures.

Cell culture and immunoblot analysis

Preosteoblasts were stimulated with recombinant human BMP2 (catalog number: 355-BM, R&D) or FGF1 (catalog number: 232-FA, R&D) depended on each experimental time course. RIPA buffer (20mM Tris-HCl, 0.1% SDS, 1% Triton X-100, 1% sodium deoxycholate) was used for preparation of cell extracts. Subsequently, cell lysates were separated by SDS-PAGE and transferred to Amersham Hybond-P membrane (GE Healthcare). Immunoblotting was performed with rabbit anti-phospho-SMAD1/5/8 (9511), rabbit anti-phospho-p44/42 MAPK (ERK1/2) (4376), rabbit anti-p44/42 MAP Kinase (4695), rabbit anti-phospho-p38 MAPK (4631), rabbit anti-p38 MAP Kinase (9212), rabbit anti-phospho-SAPK/JNK (4668), rabbit anti-SAPK/JNK (9258), rabbit anti-phospho-TAK1 (9399) and rabbit anti-TAK1 (4505), all from Cell Signaling. Mouse anti-β actin (catalog number: A-5441, Sigma) and rabbit anti-GAPDH (catalog number: 2118, Cell Signaling) were used as a loading control. Signal detection was performed by ECL western blotting detection reagents (GE Healthcare).

Treatment of animals with aqueous LDN-193189

LDN-193189 was dissolved in sterile endotoxin-free water (22). A dose of 2.5 mg of the LDN-193189 per kg body weight per day was injected intraperitoneally into pregnant mice on days E14 through E18 and continued through P15 to nursing dams.

Results

Generation of constitutively active form of Bmpr1a mice and validation of neural crest-specific Cre mice.

To target enhanced BMP signaling to the cranial neural crest (CNC) cells, we generated transgenic mice that conditionally express a constitutively active form of *Bmpr1a* (*ca-Bmpr1a*) (Fig. S2A). A mutation of Gln residue 233 to Asp (Q233D) of the glycine-serine (GS) rich kinase regulatory domain of *Bmpr1a* is known to result in constitutive activation of the type I receptor kinase activity (23). We bred these mice with *P0-Cre* mice, which express a Cre-recombinase transgene under control of a neural crest-specific promoter (24). This genetic manipulation enhances BMP signaling specifically in neural crest-derived tissues. We confirmed localization of *P0-Cre* expressing cells in the skull using ROSA26 reporter line (25) (Fig. S2). LacZ positive cells were observed in nasal-frontal bones and the metopic suture as expected (11), consistent with efficient targeting of CNC-derived cells by the *P0-Cre* transgene during skull development.

Enhanced BMP signaling through ca-BMPR1A in cranial neural crest cells causes craniosynostosis.

The mutant mice, which carried both *ca-Bmpr1a* and *P0-Cre* transgenes (*ca-Bmpr1a:P0-Cre*, or mutant (MT), hereafter), showed enhanced levels of SMAD1/5/8 phosphorylation without ligand stimulation in CNC derived-preosteoblast cells from skull that were further increased by BMP2 ligand treatment (Fig. S2B). These mutant mice displayed short broad snouts and orbital hypertelorism (Fig. 1A-D). Skeletal staining at postnatal day 17 (P17) and histological observation at P8 revealed premature fusion of the anterior frontal (AF) suture in *ca-Bmpr1a:P0-Cre*, while AF sutures in control mice retained patency (Fig. 1E-H). Other sutures including the coronal suture developed normally (Fig. S4), and no bones were missing in skull base of mutant mice (Fig. S5).

Calvaria from *ca-Bmpr1a:P0-Cre* were thinner (Fig. 1G, H), resembling a phenotype found in a mouse model of Apert syndrome harboring a mutation in *Fgfr2* (Ser252Trp) representing one of the most severe forms of craniosynostosis. Interestingly, we found evidence of increased apoptosis in mutant mice at newborn stage (Fig. S6), consistent with the thin calvaria found in *ca-Bmpr1a:P0-Cre* (Fig. *1G, H)* and in certain syndromes such as Apert type craniosynostosis (21,26-30).

Since our mutant mice showed increased levels of Smad signaling in neural crest-derived tissues including osteoblasts, one of the immediate hypotheses to be examined is that the enhanced BMP signaling in differentiated osteoblasts stimulates their proliferation and/or differentiation to ossify suture mesenchyme. Thus, first we investigated the proliferative and differentiation capability of the mutant osteoblasts. However, there were no significant differences in the ability of skull-derived pre-osteoblasts to proliferate or differentiate (Fig. S7). Next, we bred *ca-Bmpr1a* mice with *Col1-CreER*^{TM} (*ca-Bmpr1a:Col1-CreER*^{TM}) (31) to activate BMP signaling in an osteoblast-specific manner to examine if enhanced BMP signaling through BMPR1A exerts its effects through osteoblast-lineage committed cells during skull development. While *Col1-CreER*^{TM} showed the robust Cre recombination in whole skull in our previous study (31), *ca-Bmpr1a:Col1-CreER*^{TM} mice did not display any of the skull abnormalities seen in *ca-Bmpr1a:P0-Cre* mice (Fig. S8). Such striking phenotypic differences between neural crest-specific and osteoblast-specific activation of BMP signaling reveal the critical role of BMP signaling in neural crest-derived multipotent cells rather in the osteoblast-committed lineages for governing normal skull development by regulating suture patency.